

BASIC RESEARCH PAPER

## Extracellular stimulation of VSIG4/complement receptor Ig suppresses intracellular bacterial infection by inducing autophagy

Kwang H. Kim<sup>a</sup>, Beom K. Choi<sup>b</sup>, Young H. Kim<sup>c</sup>, Chungyong Han<sup>b</sup>, Ho S. Oh<sup>b</sup>, Don G. Lee<sup>b</sup>, and Byoung S. Kwon<sup>a,b,d</sup>

<sup>a</sup>Eutilex, The Catholic University School of Medicine Seoul, Korea; <sup>b</sup>Cancer Immunology Branch, Division of Cancer Biology, National Cancer Center, Goyang, Korea; <sup>c</sup>Immune Cell Production Unit, Program for Immunotherapeutic Research, National Cancer Center, Goyang, Korea; <sup>d</sup>Department of Medicine, Tulane University Health Sciences Center, New Orleans, LA, USA

### ABSTRACT

VSIG4/CR1g (V-set and immunoglobulin domain containing 4) is a transmembrane receptor of the immunoglobulin superfamily that is expressed specifically on macrophages and mature dendritic cells. VSIG4 signaling accelerates phagocytosis of C3-opsonized bacteria, thereby efficiently clearing pathogens within macrophages. We found that VSIG4 signaling triggered by C3-opsonized *Listeria* (opLM) or by agonistic anti-VSIG4 monoclonal antibody (mAb) induced macrophages to form autophagosomes. VSIG4-induced autophagosomes were selectively colocalized with the intracellular LM while starvation-induced autophagosomes were not. Consistent with these results, the frequency of autophagosomes induced by infection with opLM was lower in VSIG4-deficient bone marrow-derived macrophages (BMDMs) than in WT BMDMs. Furthermore, when VSIG4 molecules were overexpressed in HeLa cells, which are non-macrophage cells, VSIG4 triggering led to efficient uptake of LM, autophagosome formation, and killing of the infected LM. These findings suggest that VSIG4 signaling not only promotes rapid phagocytosis and killing of C3-opsonized intracellular bacteria, as previously reported, but also induces autophagosome formation, eliminating the LM that have escaped from phagosomes. We conclude that VSIG4 signaling provides an anti-immune evasion mechanism that prevents the outgrowth of intracellular bacteria in macrophages.

### ARTICLE HISTORY

Received 13 March 2015  
Revised 13 May 2016  
Accepted 24 May 2016

### KEYWORDS

autophagy; CR1g; LC3B;  
*Listeria*; macrophage;  
ubiquitin; VSIG4

### Introduction

Phagocytic cells such as macrophages serve as sentinels for the immune system against *in situ* infection:<sup>1</sup> once they encounter a pathogen, they alarm the immune system by secreting proinflammatory cytokines and chemokines.<sup>2,3</sup> Some of the phagocytic cells home to draining lymph nodes and initiate an adaptive immune response by presenting an engulfed pathogen epitope with their major histocompatibility complex (MHC) molecules.<sup>4</sup> Most phagocytosed pathogens are cleared in phagolysosomes.<sup>5</sup> Some bacteria, however, are capable of surviving by blocking the biogenesis of phagolysosomes or by escaping into the cytoplasm before the phagosomes fuse with lysosomes. For example, *Listeria monocytogenes* (LM), an intracellular bacterium that causes listeriosis, can escape from phagosomes by secreting virulence factors such as listeriolysin O (LLO) and phospholipase C,<sup>6</sup> while *Mycobacterium tuberculosis*, the causative agent of most cases of tuberculosis, prolongs its survival inside the phagosome by impeding phagosome-lysosome fusion.<sup>7</sup>

In order to control intracellular bacterial infections macrophages employ another process, ‘autophagy’. The main role of autophagy is to eliminate unwanted cell constituents such as misfolded proteins, damaged organelles, and intracellular

bacteria from the cell.<sup>8–10</sup> This allows the cell to maintain cellular homeostasis under stressful conditions including nutrient starvation. Autophagy also has a protective role against bacterial infection.<sup>11,12</sup> Antibacterial autophagy, also referred to as xenophagy, is activated by stimulation of pathogen-associated molecular pattern (PAMP) receptors such as toll-like receptors (TLRs), NOD-like receptors, RIG-I-like receptors and AIM2-like receptors.<sup>13–15</sup> Autophagy can function as a degradation system detecting microbes that invade the cytosol of the host cell, and can also modulate innate and adaptive immunity, transcriptional signatures for inflammation, and the production and secretion of cytokines including type I IFN.<sup>16, 17</sup>

VSIG4/CR1g (V-set and immunoglobulin domain containing 4) is a 50-kDa type I transmembrane receptor that is specifically expressed on monocytes, macrophages, and dendritic cells,<sup>18,19</sup> and is a receptor for the C3b cleavage product of C3 (complement component 3) and inactivated C3b (iC3b). Therefore, complement-opsonized microbes can be efficiently recognized and phagocytosed by VSIG4-expressing macrophages.<sup>18</sup> In addition, VSIG4 cross-linked by an agonistic antibody rapidly translocates to bacteria-containing phagosomes and enhances the acidification of the phagosomes before the bacteria can escape, and this process requires CLIC3 (chloride intracellular channel protein 3).<sup>20</sup> VSIG4 has been reported to

regulate T-cell proliferation *in vitro* and *in vivo*,<sup>21</sup> and a soluble form of HsVSIG4 displays therapeutic potential in mouse models of arthritis by inhibiting autoreactive immune responses.<sup>22</sup>

We have previously reported that VSIG4 signaling eliminates phagocytosed LMs by rapidly inducing CLIC3-dependent acidification of LM-containing phagosomes.<sup>20</sup> However, we also suspected that VSIG4 signaling might inhibit the intracellular growth of LMs that escaped into the macrophage cytosol, because some phagocytosed LMs manage to escape from phagosomes before VSIG4 was triggered and yet are eliminated. Indeed, we demonstrate here that some phagocytosed LMs escape from the phagosomes during the first hour of infection of macrophages, and VSIG4 triggering efficiently removes these cytosolic LMs by inducing the formation of LM-targeting autophagosomes. These results reveal that VSIG4 signals have effects that block the immune evasion mechanism of intracellular LM.

## Results

### Natural triggering of VSIG4 induces autophagosome formation in J774 cells

The C3b cleavage product of C3 (complement component 3) is a ligand for the VSIG4 receptor<sup>18</sup> and therefore, VSIG4 can be triggered by infecting macrophages with opsonized *Listeria*

*monocytogenes* (opLM) because the opsonized bacterial membrane is covered with C3b. We examined whether natural triggering of VSIG4 with opLM induced autophagosome formation in macrophages. However, we could not simply compare the effect of opLM with that of LM (as a control) because opLM were taken up more efficiently by macrophages than LM by binding to VSIG4. Consequently, colony-forming units (CFUs) or numbers of infected LM per macrophage were 2- to 3-fold higher with opLM than with LM when the cells were infected with the same multiplicity of infection (MOI) of LM (Fig. S1A and B). Since we found similar CFU or numbers of LM per cells when we used an MOI 6 of LM and MOI 2 of opLM, or MOI 10 of LM and MOI 4 of opLM (Fig. 1A), we examined autophagosome formation by infecting J774 cells with MOI 10 of LM and MOI 4 of opLM that were labeled with 5(6)-carboxytetramethylrhodamine *N*-hydroxysuccinimide ester (TMR). By intracellularly staining of MAP1LC3B/LC3B (microtubule associated protein 1 light chain 3),<sup>13</sup> we assessed autophagosome formation in the LM- and opLM-infected J774 cells. Numbers of autophagosomes > 1.5  $\mu$ m in diameter were higher in opLM-infected J774 cells than LM-infected cells (Fig. 1B, left) and statistical analysis also indicated that VSIG4 triggering significantly increased autophagosome formation (Fig. 1B, right).

Since the conversion of LC3B-I to LC3B-II is indicative of autophagic activity<sup>23</sup> we examined the conversion of LC3B-I to

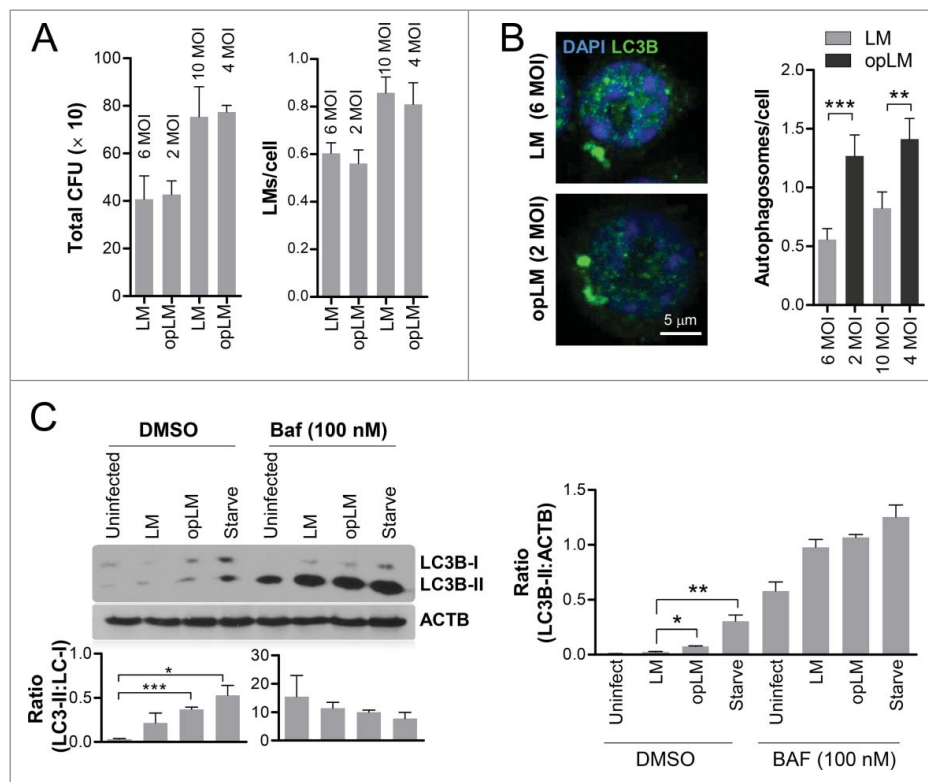


**Figure 1.** Oponized *Listeria* induces autophagosome formation in J774 cells. (A) J774 cells ( $2 \times 10^5$  cells) were infected with the indicated MOI of LM or opLM for 1 h and washed, lysed and plated on BHI agar plates to determine CFU (left). To count LM numbers per cell, J774 cells were infected with TMR-labeled LM or opLM at the indicated MOI for 1 h, washed with PBS, fixed with 4% paraformaldehyde, and visualized under a fluorescence microscope. Numbers of LM per cells were determined using the AxioVision Rel. 4.8 imaging program (right). The data shown are representative of 3 independent experiments. (B) J774 cells were infected with the indicated MOI of LM or opLM for 1 h, washed with PBS, and incubated in a 37°C CO<sub>2</sub> incubator for 2 h. The cells were fixed and stained with anti-LC3B antibody and further with anti-Oc1gG-FITC. Samples were mounted with DAPI-containing mounting solution (Vector) and visualized under a confocal microscope. Numbers of autophagosomes (LC3B<sup>+</sup>) > 1.5  $\mu$ m in diameter were assessed in randomly selected cells ( $n = 3$ , mean  $\pm$  SD; \*\*,  $P < 0.01$ ; \*\*\*,  $P < 0.001$ ). (C) J774 cells were preincubated with 100 nM BAF for 1 h and further infected with LM or opLM for further 2 h. Alternatively, J774 cells were cultured in serum-free medium for 4 h. J774 cells were lysed and western blotting was performed with antibodies specific to LC3B and ACTB. Relative levels were calculated by dividing the densitometry value for LC3B-II by the value for LC3B-I or ACTB. Data are representative of 3 independent experiments. Results are mean  $\pm$  SD (\*,  $P < 0.05$ ; \*\*,  $P < 0.01$ ; \*\*\*,  $P < 0.001$ ).

LC3B-II in J774 cells infected with LM and opLM. J774 cells incubated in serum-free medium for 4 h were used as a positive control for detecting LC3B-II,<sup>24</sup> and bafilomycin A<sub>1</sub> (BAF) was used to block degradation of the LC3B proteins by preventing fusion of autophagosomes and lysosomes.<sup>25</sup> Western blotting of LC3B showed that conversion of LC3B-I to LC3B-II was more extensive in the opLM-infected or serum-starved J774 cells than the uninfected cells, and this was not seen in the BAF-treated group due to the massive accumulation of LC3B-II (Fig. 1C, left). There was no significant difference between the LM-infected and opLM-infected cells in the relative levels of LC3B-II vs. LC3B-I, but we found more LC3B-II in the opLM-infected cells than the LM-infected cells when the LC3B-II levels were normalized to ACTB/ $\beta$ -actin (Fig. 1C, right). These results indicate that the uptake of opLM triggers VSIG4 signaling in J774 cells and leads to activation of autophagosome formation.

### Agonistic anti-VSIG4 antibody induces autophagosome formation

We next examined whether triggering VSIG4 with the agonistic form of anti-VSIG4 mAb would induce autophagosome formation. J774 cells incubated with LM for 1 h were treated with 1  $\mu$ g/ml of anti-MmVSIG4 mAb or RnIgG for 2 h, or were cultured in serum-free medium for 4 h. After staining with anti-LC3B mAb, autophagosomes were assessed using a fluorescence microscope. Large autophagic puncta (>1.5  $\mu$ m diameter) were detected in the anti-MmVSIG4 mAb-treated and serum starved J774 cells but not in the RnIgG-treated cells (Fig. 2A, left). The average numbers of autophagic puncta per 100 randomly selected cells were  $4.33 \pm 1.45$  in the RnIgG-treated cells,  $64.1 \pm 4.61$  in the anti-MmVSIG4-treated cells, and  $96.0 \pm 33.18$  in the serum-starved cells (Fig. 2A, right), indicating that treatment with anti-MmVSIG4 mAb increased autophagosome formation in LM-infected J774 cells. To examine whether anti-VSIG4 mAb increased the conversion of LC3B-I to LC3B-II, LM-infected J774 cells were treated with RnIgG or anti-MmVSIG4 mAb as described above in the presence of DMSO or BAF. LC3B immunoblotting demonstrated that treatment with anti-VSIG4 mAb and serum starvation enhanced the conversion of LC3B-I to LC3B-II compared with RnIgG treatment (Fig. 2B). Since SQSTM1/p62 can be used to monitor autophagy flux,<sup>26</sup> we also examined levels of SQSTM1. SQSTM1 was degraded when cells were treated with anti-MmVSIG4 mAb in the DMSO group but not in the BAF-treated group (Fig. 2B). To examine whether VSIG4 triggering alone is sufficient to induce autophagosome formation, J774 or THP-1 cells were treated with anti-VSIG4 mAb or control IgG without LM infection, and western blotting of LC3B and SQSTM1 was performed. Serum starvation fully converted LC3B-I to LC3B-II and decreased SQSTM1 in both cell types, and VSIG4 triggering alone or LM infection itself also increased LC3B-II and decreased SQSTM1 in both (Fig. 2C and 2D). To determine the kinetics of VSIG4-mediated conversion of LC3B-I to LC3B-II samples of anti-VSIG4-treated and LM-infected cells were immunoblotted to detect LC3B-II. This form of LC3B-II began to increase after 5 min and peaked at 60 to 120 min (Fig. 2E), indicating that autophagosome formation was directly induced by VSIG4 triggering.

BECN1/Beclin 1 is a key molecule needed for the formation of phagophores, the precursors to autophagosomes;<sup>27</sup> it is activated in the mouse when it dissociates from BCL2 and is phosphorylated at Ser91 and Ser94 sites.<sup>28</sup> Therefore, we asked whether VSIG4 triggering activates BECN1. Protein samples were prepared from LM-infected, RnIgG- or anti-MmVSIG4-treated J774 cells, and serum-starved cells. After immunoprecipitation with anti-BECN1 mAb the precipitated proteins were treated with antibodies specific to BCL2, phospho-BECN1, and BECN1. VSIG4 triggering and serum starvation clearly decreased BCL2 and increased phosphorylated BECN1 (Fig. 2F), indicating that VSIG4 triggers dissociation of BECN1 from BCL2 and increases its phosphorylation.

### VSIG4 triggering suppresses intracellular LM growth via autophagy

LM escapes rapidly from phagosomes to the cytosol in infected macrophages.<sup>6</sup> Since we treated J774 cells with anti-VSIG4 mAb 1 h after infection with LM,<sup>20</sup> we suspected that many of the phagocytosed LM would already have escaped to the cytosol. Since nevertheless the anti-VSIG4 mAb suppressed LM growth,<sup>20</sup> this implied that VSIG4 triggering also eliminated the escaped LM. To determine when the LM escaped from LM vacuoles, J774 cells were infected with FITC-labeled LM and stained with phalloidin to visualize actin-nucleated motile LM at times after LM infection.<sup>29</sup> The infected LM did not colocalize with F-actin at 0 h, which indicated that they were in phagosomes, but colocalization was evident 30 min after infection (Fig. S2A and B). About 80% of the infected LMs were phalloidin-positive by 1 h after infection, which implied that most of the infected LMs were free from phagosomes.

Since autophagy restricts the growth of a variety of intracellular pathogens,<sup>15</sup> we next examined whether VSIG4 triggering induced the formation of autophagosomes targeting the escaped LM. J774 cells were infected with TMR-labeled LM for 1 h and treated with 1  $\mu$ g/ml of control rat RnIgG or anti-MmVSIG4 for another 2 h, and other cells were simply incubated in starvation conditions for 4 h. Autophagosomes were detected by staining with anti-LC3B mAb. Autophagosomes were efficiently formed by serum starvation and by VSIG4 triggering, but colocalization of LM and autophagosomes was only increased by VSIG4 triggering (Fig. 3A). Cross scan images confirmed that red fluorescence peaks, due to LM, were located in the middle of green fluorescence peaks (LC3B) marking the autophagosomes in the anti-MmVSIG4 mAb-treated cells (Fig. 3B, low), but not in the starvation group (Fig. 3B, middle). These results indicate that the autophagosomes induced by VSIG4 signaling, but not those induced by starvation, target the escaped LM.

Like phagosomes, autophagosomes undergo a maturation process by fusing with lysosomes,<sup>25</sup> and this process is necessary for killing intracellular bacteria.<sup>30</sup> Therefore, we next examined whether VSIG4 signaling-mediated LM-containing autophagosomes fuse with lysosomes. Dual staining of LC3B and LAMP1 demonstrated that many LC3B<sup>+</sup> LMs colocalized with LAMP1 (LC3B<sup>+</sup> LAMP1<sup>+</sup> DAPI<sup>+</sup>) in the anti-MmVSIG4-treated cells but very few in the RnIgG-treated cells (Fig. 3C, left). All the fusion events were inhibited by NH<sub>4</sub>Cl, a fusion inhibitor (Fig. 3C, right).<sup>31</sup> To see

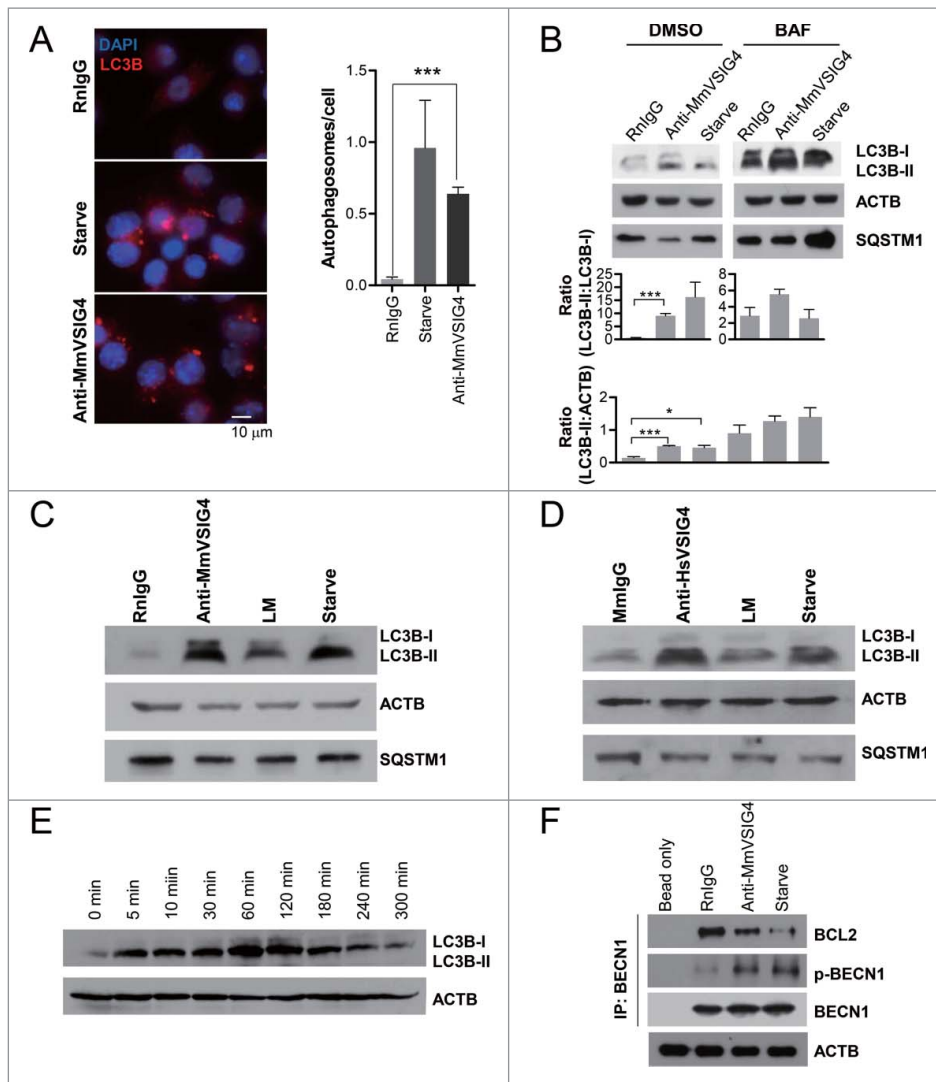


**Figure 2.** Agonistic anti-MmVSI4 mAb induces autophagosome formation. (A) J774 cells were infected with LM for 1 h, washed with PBS, and further incubated for 1 h. They were treated with 1  $\mu$ g/ml of control RnlGg or anti-MmVSI4 and incubated in a 37°C, 5% CO<sub>2</sub> incubator for 2 h. Alternatively, J774 cells were incubated in serum-free medium for 4 h without LM infection. Thereafter they were fixed with 4% paraformaldehyde, blocked with 4% BSA in PBST buffer for 40 min, stained with anti-LC3B antibody followed by anti-Oc1Gg-TMR. Samples were mounted with DAPI-containing solution, and then visualized under a fluorescence microscope. Autophagosomes (LC3B<sup>+</sup>) > 1.5  $\mu$ m in diameter were counted per 100 randomly selected cells (DAPI<sup>+</sup>) in each group (n = 3, mean  $\pm$  SD; \*\*\*,  $P < 0.001$ ). (B) LM-infected J774 cells were treated with RnlGg or anti-MmVSI4 mAb as described above, or J774 cells were cultured in serum-free medium for 4 h in the presence of DMSO or 100 nM BAF. The cells were lysed and western blotting was performed with antibodies specific for LC3B, SQSTM1 and ACTB. Relative levels were calculated as above (n = 3, mean  $\pm$  SD; \*,  $P < 0.05$ ; \*\*\*,  $P < 0.001$ ). (C) J774 cells were incubated on control RnlGg- or anti-MmVSI4-coated plates for 2 h, incubated with LM for 2 h, or serum-starved for 4 h. Then each group of cells was lysed and western blotting was performed with antibodies specific for LC3B, SQSTM1 and ACTB. (D) THP-1 cells were incubated on control MmlGg- or anti-HsVSI4-coated plates for 2 h and the same experiment was performed as in (C). (E) J774 cells were infected with LM for 1 h and further incubated for 1 h. Then the cells were treated with 1  $\mu$ g/ml of anti-MmVSI4 mAb for the indicated times. Western blotting was performed with antibodies specific for LC3B and ACTB. (F) LM-infected J774 cells were treated with RnlGg or anti-MmVSI4 mAb for 2 h, or the cells were incubated in serum-free medium for 4 h. Each group of cells was harvested, lysed and immunoprecipitated using anti-BECN1 crosslinked with Dynabead-protein G, and western blotted with anti-BCL2, anti-phosphorylated (p)-BECN1, and anti-BECN1. As a negative control, total cell lysates were immunoprecipitated with Dynabead-protein G and western blotting was performed as described above. Data are representative of 3 independent experiments.

whether recruitment of the autophagic machinery is essential for VSI4-mediated suppression of LM growth, we generated *ATG5*-knockout THP-1 (*ATG5*<sup>-/-</sup> THP-1) cells since THP-1 plays an essential role in autophagosome elongation<sup>32</sup> and used them in LM killing assays. When THP-1-mock and *ATG5*<sup>-/-</sup> THP-1 cells were infected with LM and treated with MmlGg or anti-HsVSI4 mAb as described above, the VSI4-mediated suppressive effects on LM growth were completely abolished in the absence of *ATG5* (Fig. 3D). THP-1-mock and *ATG5*<sup>-/-</sup> THP-1 cells were then infected with TMR-labeled LM, treated with MmlGg or anti-HsVSI4 mAb, and intracellularly stained with

anti-LC3B mAb to visualize autophagosomes. Confocal microscopy showed that serum starvation markedly increased autophagosome formation in the THP-1-mock cells, but that these autophagosomes did not colocalize with LM (Fig. 3E). However, VSI4 triggering again selectively increased LC3B<sup>+</sup> LMs in the THP-1-mock cells, and was not observed in the *ATG5*<sup>-/-</sup> THP-1 cells (Fig. 3E). Statistical analysis confirmed that VSI4 triggering increased LC3B<sup>+</sup> LMs in the THP-1-mock cells but not the *ATG5*<sup>-/-</sup> THP-1 cells (Fig. 3F). These data indicate that VSI4 signaling inhibits the growth of intracellular LM by inducing autophagosome-mediated LM targeting.

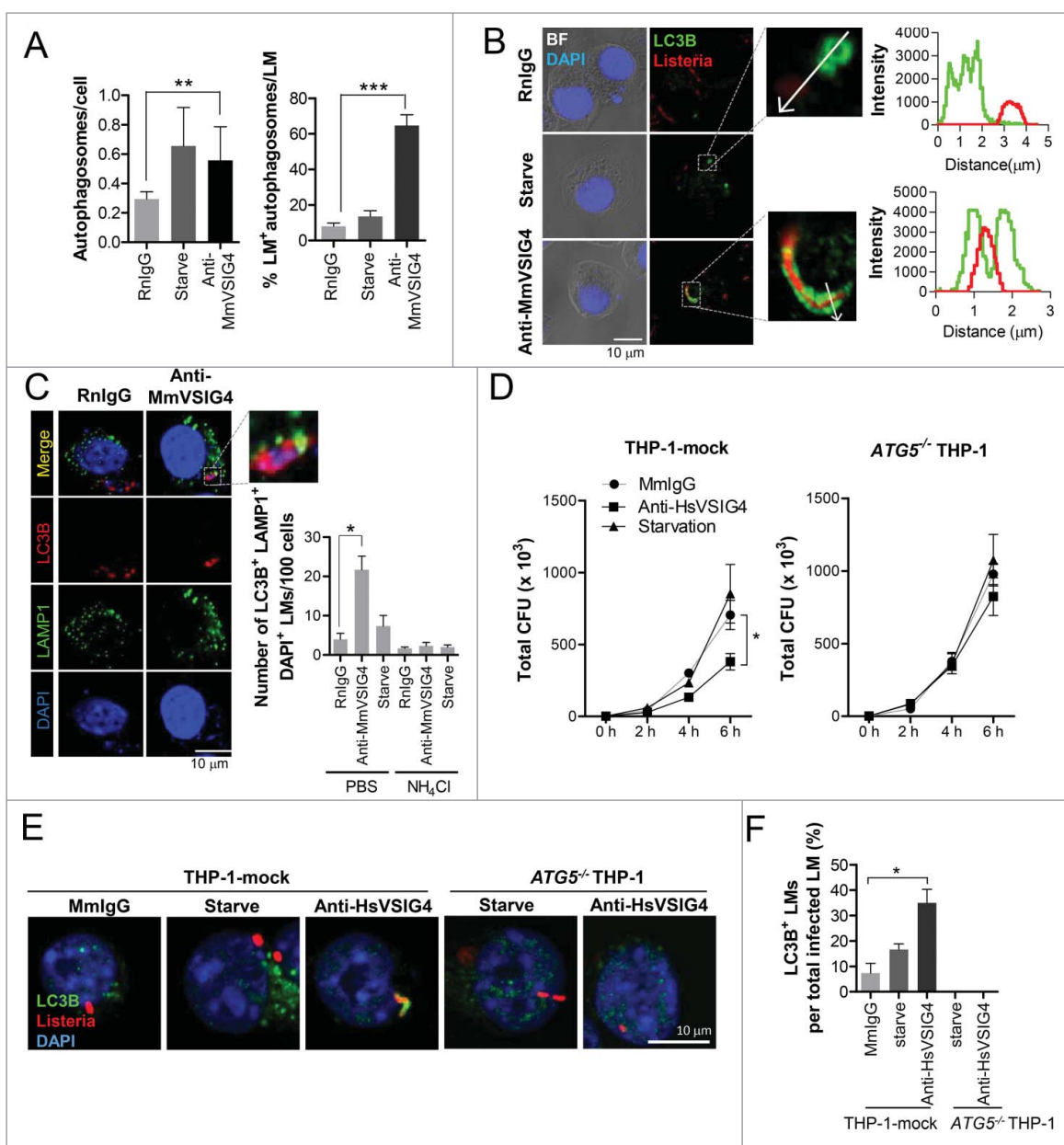


**Figure 3.** VSIG4-mediated autophagosomes suppress intracellular LM growth. (A and B) J774 cells were infected with MOI 10 of TMR-labeled LM for 1 h and further incubated for 1 h. Then the cells were treated with 1  $\mu$ g/ml of control RnlGg or anti-MmVSIG4 for 2 h as described above, or cultured in serum-free medium for 4 h. Each group of cells was fixed with PFA, stained with anti-LC3B antibody, followed by anti-Oc1gG-FITC. Samples were mounted with DAPI-containing mounting solution and visualized under a confocal microscope. Numbers of autophagosomes (over 1.5- $\mu$ m diameter) and percent of autophagosomes localizing with LM were assessed per 100 cells selected at random ( $n = 3$ , mean  $\pm$  SD; \*\*,  $P < 0.01$ ; \*\*\*,  $P < 0.001$ ) (A). Line-scan evaluation of LM and autophagosomes. Fluorescence intensities of FITC and TMR were indicated with white arrows enlarged from white dashed boxes, and displayed as intensity vs distance graphs (B). (C) J774 cells infected with MOI 10 of LM for 1 h and further incubated for 1 h. Half of the J774 cells were preincubated with 10 mM of ammonium chloride (NH<sub>4</sub>Cl) and both sets of cells were treated with 1  $\mu$ g/ml of control RnlGg or anti-MmVSIG4 for 2 h. The cells were fixed, stained with anti-LC3B antibody and anti-mouse LAMP1 and stained with anti-Oc1gG-FITC followed by anti-ChlgG-Alexa Fluor 568. Nuclei were stained with DAPI and the cells were visualized under a confocal microscope; colocalization of LM, LAMP1, and autophagosomes (LC3B<sup>+</sup> LAMP1<sup>+</sup> DAPI<sup>+</sup>) was assessed among 100 randomly selected cells. ( $n = 3$ , mean  $\pm$  SD; \*,  $P < 0.05$ ) (D) LM killing assay. THP-1-mock and ATG5<sup>-/-</sup> THP-1 cells were infected with MOI 10 of LM for 1 h, washed 3 times with PBS and further incubated for 1 h, then treated with 5  $\mu$ g/ml control MmlgG or anti-HsVSIG4 for the indicated times. CFU were assessed by plating serially diluted cell lysates on BHI agar plates. Data are representative of 3 independent experiments. Results are means  $\pm$  SDs. (\*,  $P < 0.05$ ) (E) THP-1-mock or ATG5<sup>-/-</sup> THP-1 cells were infected with MOI 10 of TMR-labeled LM for 1 h and further incubated for 1 h. Then the cells were treated with 1  $\mu$ g/ml of control MmlgG or anti-HsVSIG4 for 2 h, or cultured in serum-free medium for 4 h. Each group of cells was fixed with PFA, and stained with anti-LC3B antibody, followed by anti-Oc1gG-FITC. Samples were mounted with DAPI-containing mounting solution and visualized under a confocal microscope. (F) Percentages of autophagosomes localizing with LM were assessed per 100 cells selected at random. ( $n = 3$ , mean  $\pm$  SD; \*,  $P < 0.05$ .)

### VSIG4 signaling induces poly-ubiquitination of intracellular LM

We have provided evidence that VSIG4-mediated autophagy selectively targets intracellular LM (Fig. 3A). Therefore, we wondered how the VSIG4-induced autophagosomes could

selectively target the intracellular LM. Recent studies indicate that ubiquitin (Ub) can provide the specificity needed for selective autophagy.<sup>33</sup> Therefore, we examined whether VSIG4 signaling induced poly-ubiquitination of the LM, and whether the poly-ubiquitinated LM became localized in autophagosomes. J774 cells were infected with TMR-labeled LM for 1 h and

further treated with 1  $\mu\text{g}/\text{ml}$  of anti-MmVSIG4 mAb or control RnIgG for another 2 h, or they were serum starved for 4 h. Intracellular staining of Ub and F-actin revealed that colocalization of LM (red), F-actin (violet) and Ub (green) was barely detectable in RnIgG-treated and serum-starved J774 cells but readily observed in anti-MmVSIG4-treated cells (Fig. 4A). When the frequencies of Ub<sup>+</sup> LM among the F-actin<sup>+</sup> LM were calculated among 100 randomly selected cells, this frequency was  $\sim 10\%$  in the RnIgG-treated cells,  $\sim 40\%$  in the anti-MmVSIG4-treated cells, and  $\sim 16\%$  in the serum-starved J774 cells (Fig. 4B). Western blotting for Ub also showed that VSIG4 triggering and serum starvation reduced the amounts of Ub monomers compared with RnIgG-treated cells (Fig. 4C).

These results indicate that VSIG4 triggering selectively induces autophagosome formation via ubiquitination of escaped LMs.

### Overexpression of human VSIG4 on HeLa cells facilitates LM uptake and induces autophagosomes

Although VSIG4 triggering inhibited intracellular LM growth by inducing autophagosomes in cells of the J774 macrophage cell line, it was not clear whether this inhibition was exclusively induced by VSIG4 signaling or required additional macrophage-specific functions. We, therefore, examined VSIG4-mediated suppression of LM growth in (nonphagocytic) HeLa cells overexpressing human VSIG4 (HeLa-HsVSIG4).<sup>19</sup> We first determined the optimal MOI of LM in HeLa-mock and HeLa-HsVSIG4 cells. The HeLa cells were infected with the indicated MOI of LM or opLM for 1 h and further incubated for 1 h. When these cells were infected with LM alone for 1 h, their uptake rates were comparable (Fig. 5A, left) but uptake of opLM was  $\sim 2$ -fold higher in the HeLa-HsVSIG4 cells (Fig. 5A, right). Therefore, we infected HeLa-mock cells with MOI 4 of LM

and MOI 2 of opLM, and HeLa-HsVSIG4 cells with MOI 4 of LM and MOI 1 of opLM. Western blotting for LC3B indicated that the conversion of LC3B-I to LC3B-II was not significantly affected in the HeLa-mock cells whether they were infected with LM or opLM, whereas infection of the HeLa-HsVSIG4 cells with opLM resulted in significantly higher levels of LC3B-II than did infection with LM (Fig. 5B). Similarly, when these HeLa cells were treated with anti-HsVSIG4 mAb with or without LM infection, LC3B-II increased in the HeLa-HsVSIG4 cells but not in the HeLa-mock cells (Fig. 5C). Evidently LC3B-II accumulation in both HeLa-mock and HeLa-HsVSIG4 cells was somewhat increased by LM infection alone, and was further increased by treating the HeLa-HsVSIG4 cells with anti-HsVSIG4 mAb (Fig. 5C). SQSTM1 levels fell in serum-starved conditions as well as in opLM-infected and anti-HsVSIG4-treated HeLa-HsVSIG4 cells (Fig. 5B and C). These results indicate that VSIG4 signaling alone can induce autophagosome formation in nonphagocytic as well as phagocytic cells.

Use of the LM-killing assay demonstrated that treatment with anti-HsVSIG4 mAb suppressed LM growth substantially in HeLa-HsVSIG4 cells but not in HeLa-mock cells, or HeLa-HsVSIG4<sup>ext</sup> cells, which express HsVSIG4 without its cytoplasmic tail (Fig. 5D). To further examine whether recruitment of the autophagy equipment is essential for VSIG4-mediated suppression of LM growth even in nonphagocytic cells, we generated ATG5-knockout HeLa and HeLa-HsVSIG4 cells by deleting  $\sim 32$  base pairs of ATG5 exon 2, and designated these derivatives ATG5<sup>-/-</sup> HeLa and ATG5<sup>-/-</sup> HeLa-HsVSIG4 cells, respectively (Fig. S3). Neither of these derivatives converted LC3B-I into LC3B-II in response to serum starvation or anti-HsVSIG4 treatment (Fig. S4). Therefore, we performed LM killing assays as described above using these cells. As expected,

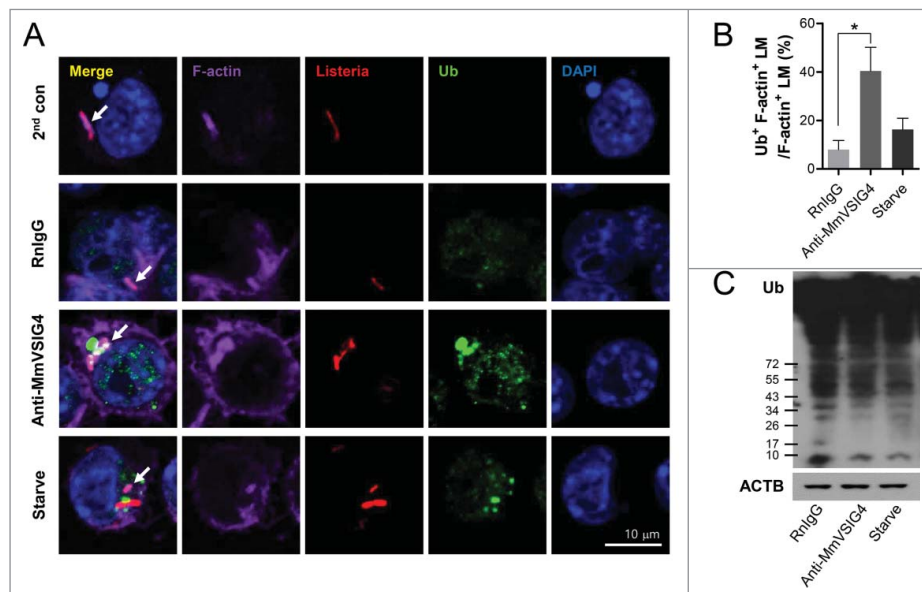


**Figure 4.** Poly-ubiquitination of LM by VSIG4 triggering. TMR-labeled LM-infected J774 cells were incubated for 1 h, treated with 1  $\mu\text{g}/\text{ml}$  of control RnIgG or anti-MmVSIG4 mAb, and incubated in a 37°C, 5% CO<sub>2</sub> incubator for 2 h or cultured in serum-free medium for 4 h. (A) The cells were fixed with 4% PFA, stained with anti-Ub mAb, followed by anti-MmIgG-FITC, and F-actin was stained with Phalloidin-Alexa Fluor 647. Samples were mounted with DAPI-containing mounting solution and visualized under a confocal microscope. (B) Percentages of F-actin<sup>+</sup> Ub<sup>+</sup> LM among the F-actin<sup>+</sup> LM were calculated among 100 randomly selected cells. ( $n = 3$ , mean  $\pm$  SD; \*,  $P < 0.05$ ) (C) Western blotting was performed with antibodies specific for ubiquitin (Ub) and ACTB. Data are representative of 3 independent experiments.

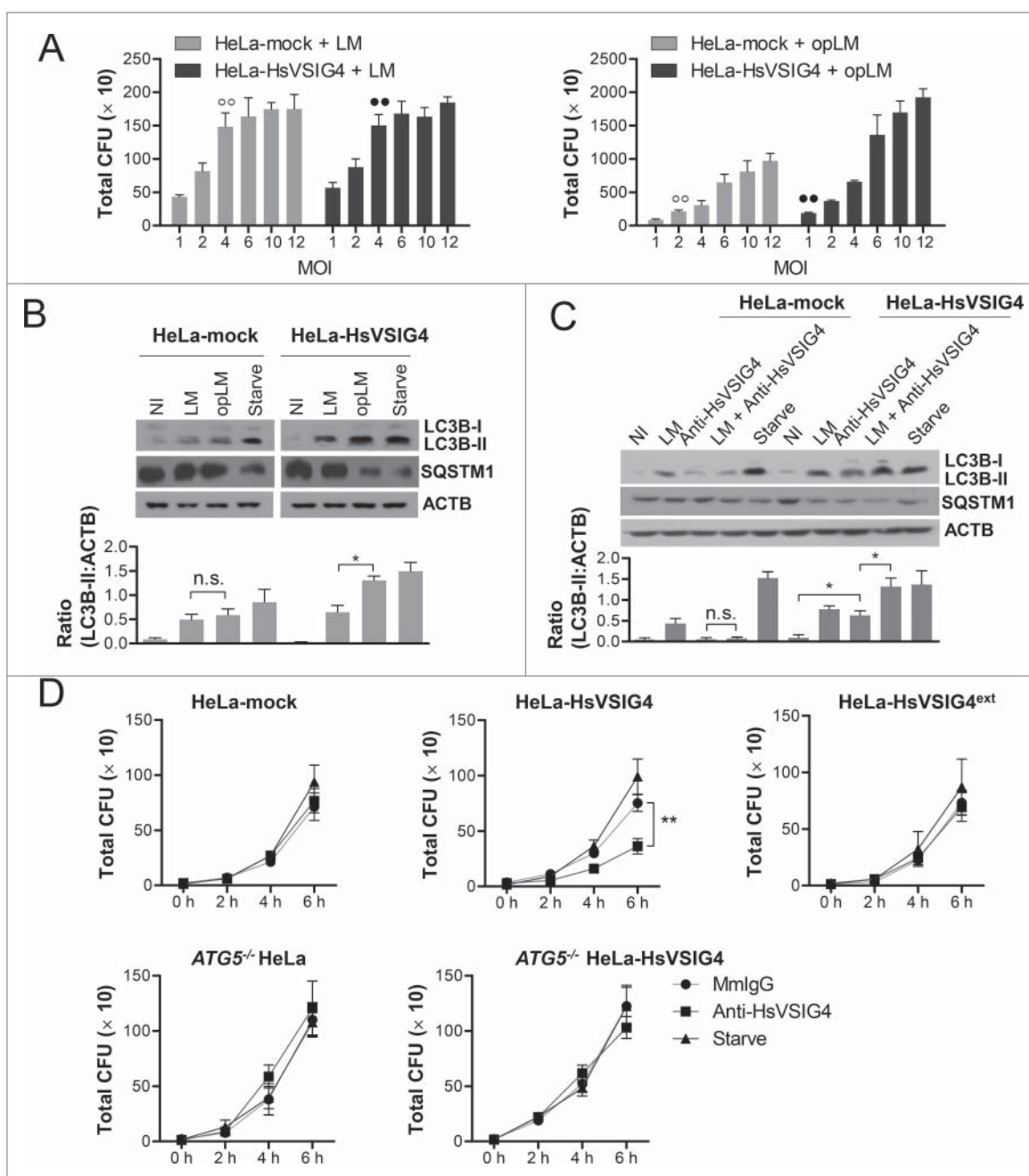


**Figure 5.** VSIG4-mediated induction of autophagosomes in human VSIG4-expressing HeLa cells. (A) HeLa-mock or human VSIG4-overexpressing HeLa (HeLa-HsVSIG4) cells were infected with various MOI of LM (left graph) or opLM (right graph) for 1 h in a 37°C, 5% CO<sub>2</sub> incubator. The infected cells were washed, lysed and plated on BHI agar plates to determine CFU. Open (○) and closed circles (●) indicate the MOI of LM or opLM that were used to equally infect HeLa and HeLa-HsVSIG4 cells in the following experiments. Data are representative of 3 independent experiments. (B) HeLa-mock cells were infected with MOI 2 of LM or MOI 2 of opLM, and HeLa-HsVSIG4 cells were infected with MOI 4 of LM or MOI 1 of opLM for 2 h. As a positive control, HeLa-mock and HeLa-HsVSIG4 cells were incubated in serum-free conditions for 4 h in a 37°C, 5% CO<sub>2</sub> incubator. Western blotting was performed with antibodies specific for LC3B, SQSTM1 and ACTB (NI, no infection). (n = 3, mean ± SD; \*, P < 0.05; \*\*, P < 0.01; \*\*\*, P < 0.001) (C) HeLa-mock and HeLa-HsVSIG4 cells were infected with MOI 4 of LM for 1 h and further incubated for 1 h. Then the cells were treated with 5 μg/ml of anti-HsVSIG4 or MmlgG for 2 h. As negative and positive controls, HeLa-mock and HeLa-HsVSIG4 cells were cultured in serum-free conditions for 4 h, or treated with anti-HsVSIG4 mAb or MmlgG without LM infection. Western blotting was performed with antibodies specific for LC3B, SQSTM1 and ACTB (n = 3, mean ± SD; \*, P < 0.05; \*\*, P < 0.01; \*\*\*, P < 0.001). (D) HeLa-mock, ATG5<sup>-/-</sup> HeLa, HeLa-HsVSIG4<sup>ext</sup> (expressing tail-less human VSIG4), HeLa-HsVSIG4 and ATG5<sup>-/-</sup> HeLa-HsVSIG4 cells were infected with LM and further incubated for 1 h. Each group of cells was treated with MmlgG or anti-HsVSIG4 mAb, or serum-starved as described above. The cells were harvested and lysed at the indicated time points, and the lysates were plated on BHI agar plates to determine CFU. Data are representative of 3 independent experiments. Results are mean ± SD (\*\*, P < 0.01).

the VSIG4-mediated suppression of LM growth was completely reversed in ATG5<sup>-/-</sup> HeLa-HsVSIG4 cells (Fig. 5D).

Taken together, these observations show that HsVSIG4 overexpression facilitates LM uptake in (nonphagocytic) HeLa cells and stimulates autophagosome formation, so inhibiting intracellular LM growth.

### **VSIG4 triggering inhibits intracellular growth of LM in bone marrow-derived macrophages by inducing autophagy**

To establish whether VSIG4 signaling induces autophagosome formation and thus inhibits intracellular LM growth in primary

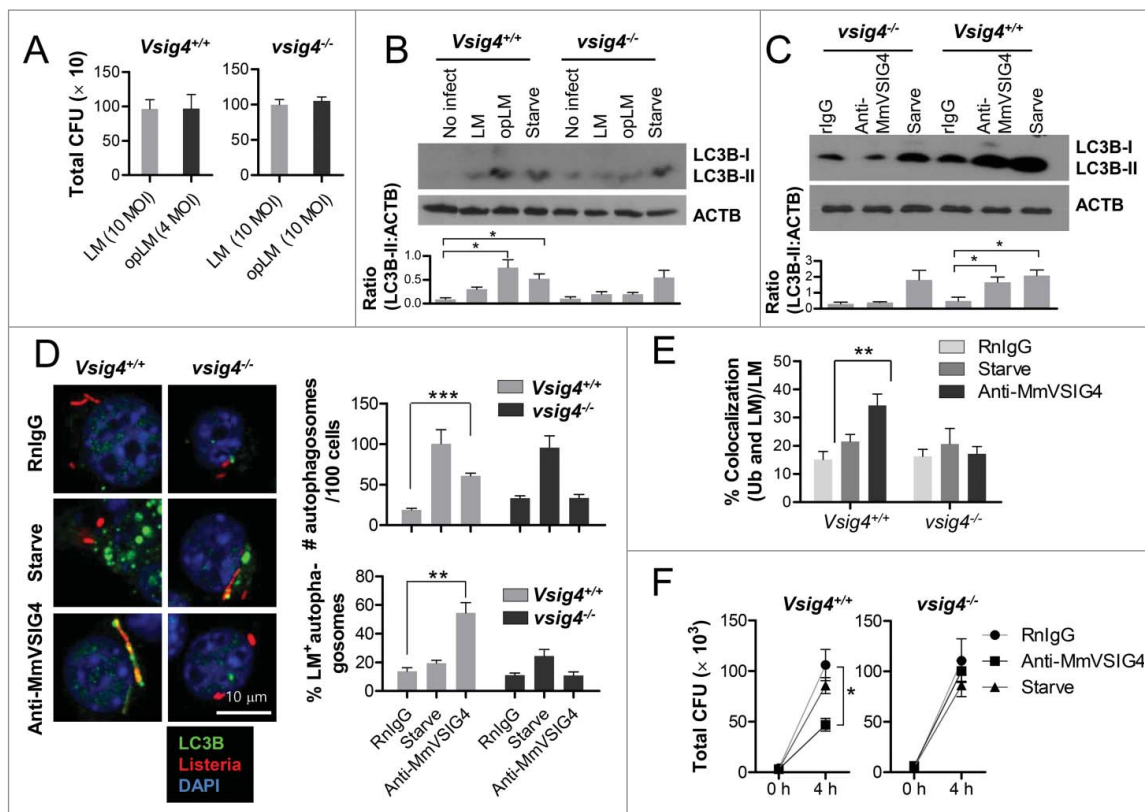


**Figure 6.** VSIG4-mediated regulation of autophagosome formation and intracellular LM growth in bone marrow-derived macrophages. (A) *Vsig4*<sup>+/+</sup> and *vsig4*<sup>-/-</sup> BMDMs were infected with the indicated MOI of LM or opLM as described above, and CFUs were determined by plating the cell lysates on BHI agar plates. (B) *Vsig4*<sup>+/+</sup> and *vsig4*<sup>-/-</sup> BMDMs were infected with LM or opLM for 1 h as described in (A), washed, and cultured for another 2 h. Alternatively, the BMDMs were cultured in serum-free conditions for 4 h. Cell lysates were prepared and western blotting was performed with antibodies specific for LC3B and ACTB ( $n = 3$ , mean  $\pm$  SD; \*,  $P < 0.05$ ). (C) *Vsig4*<sup>+/+</sup> and *vsig4*<sup>-/-</sup> BMDMs were infected with MOI 10 of LM for 1 h, washed with PBS, and further incubated for 1 h. The cells were treated with 1  $\mu$ g/ml of control RnlGg or anti-MmVSIG4 mAb for 2 h. Cell lysates were prepared and western blotting was performed with antibodies specific for LC3B and ACTB. Relative levels were calculated by dividing the densitometry values for LC3B-II by the values for ACTB ( $n = 3$ , mean  $\pm$  SD; \*,  $P < 0.05$ ). (D) *Vsig4*<sup>+/+</sup> and *vsig4*<sup>-/-</sup> BMDMs were infected with MOI 10 of TMR-labeled LM for 1 h and further incubated for 1 h. Then they were treated with 1  $\mu$ g/ml of control RnlGg or anti-MmVSIG4 for 2 h, or cultured in serum-free medium for 4 h. LC3B was intracellularly stained and visualized under a confocal microscope as described above. Numbers of autophagosomes (over 1.5- $\mu$ m diameter) and percentages of autophagosomes that colocalized with LM were assessed from 100 randomly selected cells ( $n = 3$ , mean  $\pm$  SD; \*\*,  $P < 0.01$ ; \*\*\*,  $P < 0.001$ ). (E) *Vsig4*<sup>+/+</sup> and *vsig4*<sup>-/-</sup> BMDMs were infected with TMR-labeled LM and further incubated for 1 h. The cells were treated with anti-MmVSIG4 mAb or RnlGg for another 2 h. Ub was intracellularly stained and visualized under a confocal microscope. Percentages of colocalization of Ub and LM were calculated among 100 randomly selected cells ( $n = 3$ , mean  $\pm$  SD; \*\*,  $P < 0.01$ ). (F) *Vsig4*<sup>+/+</sup> and *vsig4*<sup>-/-</sup> BMDMs were infected with MOI 10 of LM for 1 h, washed, and further incubated for 1 h. Then they were treated with 5  $\mu$ g/ml of control RnlGg or anti-MmVSIG4 mAb, or incubated in serum free condition. CFU were assessed by plating cell lysates on BHI agar plate. Data are representative of 3 independent experiments. Results are mean  $\pm$  SD (\*,  $P < 0.05$ ).

macrophages, we isolated bone marrow-derived macrophages (BMDMs) from *Vsig4*<sup>+/+</sup> and *vsig4*<sup>-/-</sup> C57BL/6 mice.<sup>18</sup> We first normalized numbers of LM taken up by the 2 strains, *Vsig4*<sup>+/+</sup> and *vsig4*<sup>-/-</sup> BMDM, and found that opsonization of LM increased LM uptake rate 2.5 fold more in the *Vsig4*<sup>+/+</sup> BMDMs than in the *vsig4*<sup>-/-</sup> BMDMs (Fig. 6A). Western blotting of LC3B demonstrated that LC3B-II increased after infection of *Vsig4*<sup>+/+</sup> BMDMs with opLM, but not with LM alone or after infection of *vsig4*<sup>-/-</sup> BMDMs (Fig. 6B). VSIG4 triggering with anti-MmVSIG4 mAb also increased LC3B-II in LM-infected *Vsig4*<sup>+/+</sup> BMDMs (only), and the level of LC3B-II produced was comparable to that of serum-starved BMDMs (Fig. 6C).

We also assessed autophagosome formation in TMR-labeled LM-infected BMDMs by staining intracellular LC3B as described above. Autophagosome formation was significantly increased by serum starvation in both *Vsig4*<sup>+/+</sup> and *vsig4*<sup>-/-</sup> BMDMs, but it was triggered by VSIG4 in *Vsig4*<sup>+/+</sup> BMDMs only (Fig. 6D, upper). LM-containing autophagosomes were only increased by VSIG4 triggering not by serum starvation

(Fig. 6D, lower), showing once again that serum starvation induces autophagosome formation nonspecifically, whereas VSIG4 selectively induces autophagosome formation around the intracellular LM. We also examined the poly-ubiquitination of intracellular LM in BMDMs after VSIG4 triggering. *Vsig4*<sup>+/+</sup> and *vsig4*<sup>-/-</sup> BMDMs were infected with TMR-labeled LM and further treated with RnlGg or anti-MmVSIG4 mAb, or cultured in serum-free medium, as described before. Intracellular staining of Ub showed that colocalization of LM and Ub was significantly increased by VSIG4 triggering, but not by serum starvation or in the *vsig4*<sup>-/-</sup> BMDMs (Fig. 6E).

To see whether VSIG4 triggering in BMDMs would inhibit the intracellular growth of escaped LM, *Vsig4*<sup>+/+</sup> and *vsig4*<sup>-/-</sup> BMDMs were infected with MOI 10 of LM for 1 h, washed and cultured for another 1 h to allow escape of LM into the cytosol, followed by exposure to RnlGg or anti-MmVSIG4 mAb. VSIG4 triggering suppressed LM growth substantially more in the *Vsig4*<sup>+/+</sup> BMDMs than in the RnlGg-treated or serum-starved *Vsig4*<sup>+/+</sup> BMDMs, and growth suppression did not occur in the *vsig4*<sup>-/-</sup> BMDMs (Fig. 6F).



Taken together, our data indicate that VSIG4 triggering in primary BMDMs induces the formation of LM-targeting autophagosomes and these neutralize the escape mechanism of the LM.

## Discussion

In this study, we have shown that extracellular stimulation of macrophages with VSIG4 activates an autophagy mechanism that removes LM that have escaped from phagosomes. Polyubiquitination of the LM is an important aspect of this mechanism as it promotes the selective induction of autophagosomes around the marked bacteria. We also showed that transgenic expression of VSIG4 in cells of the nonphagocytic HeLa cell line cells allows them to take up opsonized LM and selectively target autophagosomes to LM. Our findings demonstrate that VSIG4 signals provide 2 defense mechanisms against intracellular bacterial infections: 1) phagosome-dependent defense involving uptake of the circulating complement-opsonized pathogens and rapid acidification of the phagosomes, as previously reported,<sup>20</sup> and 2) xenophagy-dependent defense by selectively inducing autophagosomes directed against LM that have escaped from phagosomes.

LM deploys several virulence proteins to evade autophagic attack by host cells. InlK recruits MVP (major vault protein) to disguise its intracytosolic forms and evade autophagic recognition,<sup>34</sup> ActA recruits the ARPC (actin related protein 2/3 complex) controlling actin-based motility,<sup>35</sup> and PlcA/PlcB causes stalling of phagophores.<sup>36</sup> In MDCK cells infected with wild-type LM, no more than 10% of the cytosolic bacteria are LC3B positive at 2 h after infection.<sup>37</sup> Although it has been reported that serum starvation-induced autophagy suppresses intracellular BCG (*Mycobacterium bovis*) and *Mycobacterium tuberculosis* infection,<sup>38</sup> starvation-mediated autophagy did not suppress LM growth in THP-1, BMDMs, and HeLa-HsVSIG4 cells under our experimental conditions (Figs. 3D, 5D, and 6F). Autophagosome formation was more effectively induced by serum starvation than by anti-VSIG4 treatment (Fig. 2A), but the number of intracellular LM-targeting autophagosomes was markedly increased only by VSIG4 triggering and not by serum starvation (Fig. 3A and B). This phenomenon can be explained by supposing that LM evades autophagic recognition by expressing ActA, InlK, and PlcA/PlcB, and that this is somehow inhibited by VSIG4-mediated signaling but not by serum starvation. Autophagy is also generally activated by signals evoked by stimulation of PAMP sensors such as TLRs and NOD-like receptors,<sup>11,13,15</sup> and PAMP signal-mediated autophagy is specific to intracellular forms.<sup>39</sup> In response to TLR stimulation, the adaptor protein MYD88 dissociates BCL2 from BECN1 by phosphorylating the latter<sup>40</sup> and the class III phosphatidylinositol 3-kinase complex is formed and initiates autophagy.<sup>41</sup> Meanwhile, the invading microbes are tagged by ubiquitin and associate with the receptor protein SQSTM1. Thereafter the Ub-tagged microbes are captured by PAMP-mediated autophagosomes. Although intracellular signaling via VSIG4 is poorly understood, it acts against intracellular bacteria by rapidly inducing the acidification of phagosomes<sup>20</sup> and activating the transcription factor NFκB RELA/p65.<sup>42</sup> We have also observed that VSIG4-mediated autophagosome formation

is impaired in *myd88*<sup>-/-</sup> BMDMs (data not shown). This means that the antibacterial VSIG4 signal also requires MYD88, the adapter protein for PAMP receptors.<sup>43</sup> Indeed, LM infection itself stimulated conversion of LC3B-I to LC3B-II in HeLa-mock and HeLa-HsVSIG4 cells, and this was further enhanced by treating with anti-HsVSIG4 mAb (Fig. 5C). Therefore, it seems that VSIG4 and PAMP signals cooperate to remove escaped LM, which suggests that VSIG4 triggering via TLR signals may be a key mechanism by which the antiautophagic functions of the escaped LM are neutralized.

Although we found that the uptake of opLM through VSIG4 induced autophagosome formation in macrophages (Fig. 1), it was not clear whether the autophagosome induction was mainly induced by VSIG4 signals or required additional signaling. In macrophages LM might be uptaken by the direct phagocytosis and Fc receptor- or VSIG4 receptor-mediated endocytosis. In this regard, whether VSIG4 signal alone is sufficient for the activation of autophagy or other additional signals generated during phagocytosis are also involved in activating autophagy needs to be elucidated. To address this issue, we overexpressed VSIG4 in the nonphagocytic HeLa cells to selectively uptake the opLM via VSIG4 molecule but not phagocytose them, and found that VSIG4-mediated endocytosis of opLM efficiently induced the autophagosome formation targeting the escaped LM (Fig. 5B). Moreover, treatment with agonistic anti-VSIG4 mAb alone efficiently induced autophagosome formation in HeLa-HsVSIG4 cells and in LM infection itself (Fig. 5C). In addition, opLM enter HeLa cells much more efficiently than LM, even in the absence of HsVSIG4 (Fig. 5A), suggesting that HeLa cell surface receptors recognize opsonins. Among the latter, CD46, a complement regulatory protein, has been reported to induce autophagy upon engagement, and seems to facilitate the entrance of opLM into HeLa cells.<sup>44</sup> These results indicate that the VSIG4 signal alone is potent enough to induce autophagosome formation.

VSIG4 functions as a negative regulator of T cells by inhibiting their proliferation and production of IL2<sup>21</sup> and indeed, VSIG4-expressing macrophages promote lung cancer development in a mouse model.<sup>45</sup> VSIG4 molecules appear to be expressed on the surface of resident macrophages in peripheral tissues including the liver, and they disappear after macrophage activation.<sup>21</sup> Consequently, immature macrophages in local tissues control unwanted immune responses by suppressing T cell activation via VSIG4. Thus, at the beginning of a bacterial infection, macrophages facilitate phagocytosis of the bacteria via VSIG4 but may not be effective in inducing adaptive immunity because of the VSIG4-mediated suppression of T cells. However, macrophages will be activated during the uptake of bacteria, while VSIG4 expression will decrease due to TLR signals, and adaptive immunity may be more rapidly and efficiently induced by presentation of the swiftly accumulated bacterial antigens to T cells. Therefore, VSIG4 molecules seem to turn macrophages into professional antigen-presenting cells for intracellular pathogen antigens by promoting the uptake of pathogens in the immature state and facilitating T cell priming in the activated state.

Intracellular bacteria generally neutralize the phagolysosomal activity of macrophages in order to survive. Our study

provides clear evidence that VSIG4 signaling generates a mechanism preventing the immune evasion by intracellular bacteria in macrophages. Moreover, since macrophages need to be rapidly able to present bacterial antigens, VSIG4 molecules, by facilitating the uptake and intracellular killing of opsonized pathogens, are not only crucial for the immediate early defense against intracellular bacterial infection, but are also important in inducing adaptive immune responses.

## Materials and methods

### Animals

C57BL/6 mice were purchased from Orient, Inc., Korea and the *vsig4*<sup>-/-</sup> mice on a C57BL/6 background were a kind gift from Dr. M. van Lookeren Campagne (Genentech). All animal experiments were reviewed and approved by the Animal Care and Use Committee of the National Cancer Center (NCC-10-080), and were performed in accordance with the Guide for the Care and Use of Laboratory Animals.

### Cells

J774, THP-1 and HeLa cells were purchased from ATCC (ATCC<sup>®</sup> TIB-67<sup>™</sup>, ATCC<sup>®</sup> TIB-202<sup>™</sup>, and ATCC<sup>®</sup> CCL-2<sup>™</sup>, respectively). HsVSIG4 stably expressing HeLa cells were generated as described previously.<sup>19</sup> In brief, full-length *VSIG4* was amplified by PCR using the first-strand cDNA of THP-1 cells and a specific primer set (forward including BamHI: 5'-CGG GAT CCG AAT TCG GTA CCC GTC CCA TCC TGG AAG TGC CAG AG-3' and reverse including NotI: 5'-AAG GAA AAA AGC GGC CGC TTA ACA GAC ACT TTT GCC CTC AGT-3'). The PCR products were subcloned into the mammalian expression vector pcDNA3.1 (Invitrogen, V790-20) using BamHI and NotI restriction enzyme sites. For generating a stable cell line, HeLa cells were transfected with the DNA construct using a calcium phosphate coprecipitation technique. Ten micrograms of DNA construct were incubated in 1 ml of 21 mM HEPES-NaOH, pH 6.95, 138 mM NaCl, 5 mM KCl, 0.7 mM Na<sub>2</sub>HPO<sub>4</sub>, 5.5 mM glucose, 100 mM CaCl<sub>2</sub> for 30 min at room temperature. The DNA mixture was added to 5 × 10<sup>6</sup> HeLa cells in a 10-cm dish and incubated for 3 h. After incubation, the medium was replaced with 10 ml of fresh Dulbecco modified Eagle medium (DMEM; Life Technologies, 11995040) with 10% fetal bovine serum. Transfected HeLa cells were selected with 1 mg/ml of G418 (Invitrogen, 11811031) containing DMEM medium for 1 mo.

Expression of VSIG4 on J774, THP-1 and transfected HeLa cells was detected with a FACS Calibur flow cytometer (BD FACSCalibur<sup>™</sup>; BD Bioscience, San Diego, CA). Hybridomas producing monoclonal antibodies to HsVSIG4 and MmVSIG4 were generated by immunizing Balb/c and Sprague Dawley rats with HsVSIG4- and MmVSIG4-transfected HeLa cells, respectively, as described previously.<sup>19</sup>

### Reagents

The following were used as antibodies and reagents: anti-LC3B (Cell Signaling Technology, 2775), anti-ubiquitin (P4D1; Enzo Life Sciences, BML-PW0930-0100), anti-ACTB (Santa Cruz

Biotechnology, sc-47778), anti-BECN1 (Cell Signaling Technology, 3495), anti-phospho-BECN1 (Cell Signaling Technology, 13825), anti-rabbit Alexa Fluor 488 (Invitrogen, A-11034), goat anti-rabbit rhodamine conjugate (Millipore, 12-510), 5(6)-carboxytetramethylrhodamine *N*-hydroxysuccinimide ester (TMR; Sigma Aldrich, C4759), paraformaldehyde (PFA; Sigma Aldrich, P6148), bafilomycin A<sub>1</sub>/BAF (Abcam, ab120497), poly-L-lysine (Sigma Aldrich, P8920), protease inhibitor mixture (Roche Diagnostics, 11697498001), phosphatase inhibitor cocktail (Roche Life Science, 04906845001), phalloidin-rhodamine (Invitrogen, R415), phalloidin-alexa fluor 647 (Cell Signaling Technology, 8940), anti-SQSTM1 (Cell Signaling Technology, 5114), anti-mouse LAMP1 (R&D systems, MAB4320), anti-goat IgG-Alexa Fluor 568 (Invitrogen, A-11079), donkey anti-rabbit-HRP (Santa Cruz Biotechnology, sc-2313), goat anti-mouse-HRP (Jackson ImmunoResearch, 115-035-062), ampicillin (Sigma Aldrich, A0166), brain heart infusion broth (BD Bioscience, 256110) and ammonium chloride (Sigma Aldrich, 254134).

### Listeria opsonization and infection

LM (strain 10403S; ATCC, ATCC<sup>®</sup> 35152<sup>™</sup>) was passaged in mice to maintain virulence, and cultured in brain heart infusion (BHI) broth. LM were opsonized with normal serum as previously described.<sup>46</sup> In brief, 1 × 10<sup>9</sup> CFU of LM were incubated with 200 μl of normal murine serum (C57BL/6) for 60 min at room temperature with rotation. Opsonized LM (opLM) were harvested by centrifugation at 4.5 rcf for 10 min and washed 3 times with 1 × PBS (2.7 mM KCl, 2 mM KH<sub>2</sub>PO<sub>4</sub>, 137 mM NaCl, 8.2 mM Na<sub>2</sub>HPO<sub>4</sub>·7H<sub>2</sub>O, pH 7.4). To measure numbers of internalized LM, 2 × 10<sup>5</sup> J774, THP-1, or HeLa cells were plated on 12-well culture plates, incubated with LM or opLM (MOI 2, 4, 6, 8, 10 and 12) for 1 h in a 37°C, 5% CO<sub>2</sub> incubator, washed with PBS 3 times, and exposed to a high dose of ampicillin (300 μg/ml) for 15 min to remove free LM. The cells were harvested, washed with PBS, and lysed in 1 ml of water, and serial dilutions of the lysates were plated on BHI agar.

### Immunoblot analysis

Cells were pelleted and lysed in lysis buffer (50 mM HEPES, pH 7.5, 1% Nonidet P-40 [Sigma Aldrich, 9002-93-1], 0.5% sodium deoxycholate [Sigma Aldrich, 302-95-4], 150 mM NaCl, 1 mM EDTA, 0.1 mM sodium vanadate, protease inhibitor mixture and phosphatase inhibitor cocktail) for 30 min on ice and spun at 16,100 × g for 15 min at 4°C. Cell (50 μg of total proteins) were run on SDS PAGE, transferred to PVDF membranes (Millipore, IPVH00010) and developed with antibodies against LC3B, SQSTM1, BECN1, phospho-BECN1, BCL2, ubiquitin, and ACTB. Bound antibodies were reacted with secondary HRP-Ab and detected by ECL (GE Healthcare, RPN2232). For immunoprecipitation, anti-BECN1 antibody was cross-linked with Dynabeads<sup>®</sup> protein G (Invitrogen, 10003D) and total cell lysates were incubated with antibody-crosslinked Dynabeads overnight at 4°C. Cell lysates were washed 3 times with lysis buffer and immunoblotting was performed as described above.

### Detection of autophagosomes

THP-1 or J774 cells were incubated overnight on silane-coated glass slides in a 37°C, 5% CO<sub>2</sub> incubator. They were infected with MOI 10 of LM for 1 h, washed with PBS 3 times, and further incubated for 1 h. Next they were treated with 1 µg/ml of control RnIgG or anti-MmVsig4 for 2 h or serum starved for 4 h. Each group of cells was fixed with PFA buffer (4% paraformaldehyde in 0.1 M sodium phosphate, pH 7.4) for 15 min and blocked with 4% BSA (Sigma Aldrich, 9048-46-8) in PBST (2.7 mM KCl, 2 mM KH<sub>2</sub>PO<sub>4</sub>, 137 mM NaCl, 8.2 mM Na<sub>2</sub>HPO<sub>4</sub>·7H<sub>2</sub>O, pH 7.4, 0.05% Tween 20 [Sigma Aldrich, 9005-64-5]) then incubated with anti-LC3B antibody in PBST overnight at 4°C and washed with PBST 3 times. The cells were then stained with secondary anti-OcIgG-FITC and visualized by confocal microscopy (LSM 510 Meta; Carl Zeiss, Oberkochen, Germany) or fluorescence microscopy (Observer Z1; Carl Zeiss, Oberkochen, Germany). To determine colocalization of LM and autophagosomes, J774 cells were infected with MOI 10 of TMR-labeled LM followed by IFC, as described above. Percentages of LM<sup>+</sup> autophagosomes were calculated.

### Phalloidin assay

J774 or THP-1 cells were infected with FITC-labeled LM (MOI 10) for various times in a 37°C, 5% CO<sub>2</sub> incubator. Each group of cells was fixed with PFA buffer for 15 min and blocked with 4% BSA in PBST. The fixed cells were then treated with phalloidin-rhodamine for 2 h at room temperature, washed with PBST 3 times, mounted with DAPI, and analyzed by confocal microscopy (LSM 510 Meta; Carl Zeiss, Oberkochen, Germany). LMs escaped from phagosomes were counted as phalloidin-LM double-positive LM.

### LM killing assay

LM was passaged in mice to maintain virulence, and cultured in BHI broth. For in vitro LM killing assays,<sup>19</sup> samples of 2 × 10<sup>5</sup> cells were plated on 12-well culture plates and incubated with LM (10 MOI) for 1 h at 37°C. The cells were washed with PBS, and exposed to a high concentration of ampicillin (300 µg/ml) for 15 min to remove free LM, and further incubated for 1 h. The infected cells were then treated with 5 µg/ml anti-Vsig4 or control IgG, or serum starved in a 37°C, 5% CO<sub>2</sub> incubator for 0, 2, 4 or 6 h. The cells were lysed in 1 ml of water, and serial dilutions of the lysates were plated on BHI agar.

### Generation of ATG5 KO cell lines

The Cas9/CRISPR system was used to generate ATG5 KO cell lines as previously described.<sup>47,48</sup> Briefly, ATG5-specific sgRNA expression vectors (pRGEN\_Human-ATG5\_U6\_SG\_1 and pRGEN\_Human-ATG5\_U6\_SG\_3), and a codon-optimized Cas9 expression vector (pRGEN-Cas9-CMV), were designed and purchased from ToolGen (Seoul, Korea). The 2 sgRNA expression vectors were generated to delete ATG5 by inducing dual double-strand breaks. pRGEN-Cas9-CMV and the 2 sgRNA expression vectors were transfected into HeLa and HeLa-HsVsig4 cells on day 1. On

day 4, the transfected cells were detached from the plates and cloned by limiting dilution. Expanded clones (14 clones for HeLa-mock and 16 clones for HeLa-HsVsig4) were tested for autophagy deficiency by examining conversion of LC3B-I to LC3B-II (Fig. S3). To confirm the deletion of ATG5 in the isolated ATG5 KO cell lines, ATG5<sup>-/-</sup> HeLa, ATG5<sup>-/-</sup> HeLa-HsVsig4, genomic DNA (gDNA) was extracted from each and ATG5 (NCBI accession ID: 1974) exon 2 was amplified by nested PCR. Primers ATG5-gDNA-1st\_Fwd (5'-GGCAGGGGTAAATGCGAGAATG-3') and ATG5-gDNA-1st\_Rev (5'-CACACCTGCAAGTCTATGTGCAA-3') were used for the first PCR amplification, and ATG5-gDNA-2nd\_Fwd (5'-GCTTGAAAGACTGATGCAGATACAG-3') and ATG5-gDNA-2nd\_Rev (5'-TCGTGTGTGTGTATGTGTGCAT-3') for the nested PCR. The amplified products were cloned into vectors by pGEM-Teasy Vector System (Promega, A1380), and 8 DNA clones from ATG5<sup>-/-</sup> HeLa and ATG5<sup>-/-</sup> HeLa-HsVsig4 were sequenced (Fig. S3).

### Generation of BMDMs

Femurs were obtained from 6-wk-old *Vsig4*<sup>+/+</sup> and *vsig4*<sup>-/-</sup> mice. They were placed in 60% ethanol for 1 min under a tissue culture hood and washed with PBS. The epiphyses of the bones were removed with sterile scissors and the bone marrow was flushed out with a 26G needle syringe filled with PBS. BM were centrifuged at 494 × g for 5 min and resuspended in BM culture medium (Dulbecco's modified Eagle's medium, 10% fetal bovine serum, 10 ng of CSF1/ml, 100 µg of streptomycin/ml and 100 U of penicillin/ml). The cells were then plated on Petri dishes and cultured in a 37°C, 5% CO<sub>2</sub> incubator for 3 d. The plates were rinsed with PBS, and the BM medium in them was changed and the cells were cultured for another 3 d.

### Statistical analysis

All data were analyzed with the statistical program Prism4.0 GraphPad (San Diego, CA). A Student *t* test was used to determine the statistical significance of differences between groups.

### Abbreviations

ActA	actin assembly-inducing protein
ARPC	actin related protein 2/3 complex
ATG5	autophagy-related 5
BHI	brain heart infusion
BMDM	bone marrow-derived macrophage
BAF	bafilomycin A <sub>1</sub>
C3	complement component 3, CFU, colony-forming unit
CLIC3	chloride intracellular channel protein 3
CSF1/M-CSF	colony stimulating factor 1
iC3b	inactivated complement component 3b
FITC	fluorescein isothiocyanate
gDNA	genomic DNA
IP	immunoprecipitation
LAMP1	lysosomal-associated membrane protein 1
LLO	listeriolysin O
LM	<i>Listeria monocytogenes</i>

MAP1LC3B/LC3B	microtubule-associated protein 1 light chain 3 $\beta$
mAb	monoclonal antibody
MHC	major histocompatibility complex
MOI	multiplicity of infection
MVP	major vault protein
opLM	opsonized <i>Listeria monocytogenes</i>
PAMP	pathogen-associated molecular pattern
PBS	phosphate-buffered saline
PFA	paraformaldehyde
sgRNA	short guide RNA
TLR	toll-like receptor
TMR	5(6)-carboxytetramethylrhodamine N-hydroxysuccinimide ester
Ub	ubiquitin
VSIG4	V-set and immunoglobulin domain containing 4

## Disclosure of potential conflict of interests

No potential conflicts of interest were disclosed.

## Acknowledgments

We thank Dr. Menno van Lookeren Campagne for providing VSIG4<sup>-/-</sup> mice, and Mi-Ae Kim for her help with confocal microscopy.

## Funding

This work was supported by the research grants from the National Cancer Center, Korea (NCC-1032160-5) and the National Research Foundation of Korea (NRF) funded by the Ministry of Education of Korea (NRF-2005-0093837).

## References

- [1] Hoebe K, Janssen E, Beutler B. The interface between innate and adaptive immunity. *Nat Immunol* 2004; 5:971-4; PMID:15454919; <http://dx.doi.org/10.1038/ni1004-971>
- [2] Zychlinsky A, Fitting C, Cavaillon JM, Sansonetti PJ. Interleukin 1 is released by murine macrophages during apoptosis induced by *Shigella flexneri*. *J Clin Invest* 1994; 94:1328-32; PMID:8083373; <http://dx.doi.org/10.1172/JCI117452>
- [3] Irving SG, Zipfel PF, Balke J, McBride OW, Morton CC, Burd PR, Siebenlist U, Kelly K. Two inflammatory mediator cytokine genes are closely linked and variably amplified on chromosome 17q. *Nucleic Acids Res* 1990; 18:3261-70; PMID:1972563; <http://dx.doi.org/10.1093/nar/18.11.3261>
- [4] Unanue ER. Antigen-presenting function of the macrophage. *Annu Rev Immunol* 1984; 2:395-428; PMID:6242349; <http://dx.doi.org/10.1146/annurev.iv.02.040184.002143>
- [5] Vieira OV, Botelho RJ, Rameh L, Brachmann SM, Matsuo T, Davidson HW, Schreiber A, Backer JM, Cantley LC, Grinstein S. Distinct roles of class I and class III phosphatidylinositol 3-kinases in phagosome formation and maturation. *J Cell Biol* 2001; 155:19-25; PMID:11581283; <http://dx.doi.org/10.1083/jcb.200107069>
- [6] Geoffroy C, Gaillard JL, Alouf JE, Berche P. Purification, characterization, and toxicity of the sulfhydryl-activated hemolysin listeriolysin O from *Listeria monocytogenes*. *Infect Immun* 1987; 55:1641-6; PMID:3110067; <http://iai.asm.org/content/55/7/1641.long>
- [7] Goren MB, D'Arcy Hart P, Young MR, Armstrong JA. Prevention of phagosome-lysosome fusion in cultured macrophages by sulfatides of *Mycobacterium tuberculosis*. *Proc Natl Acad Sci U S A* 1976; 73:2510-4; PMID:821057; <http://www.pnas.org/content/73/7/2510.full.pdf>
- [8] Ravikumar B, Duden R, Rubinsztein DC. Aggregate-prone proteins with polyglutamine and polyalanine expansions are degraded by autophagy. *Hum Mol Genet* 2002; 11:1107-17; PMID:11978769; <http://dx.doi.org/10.1093/hmg/11.9.1107>
- [9] Cuervo AM, Bergamini E, Brunk UT, Droge W, Ffrench M, Terman A. Autophagy and aging: the importance of maintaining "clean" cells. *Autophagy* 2005; 1:131-40; PMID:16874025; <http://dx.doi.org/10.4161/auto.1.3.2017>
- [10] Birmingham CL, Smith AC, Bakowski MA, Yoshimori T, Brumell JH. Autophagy controls Salmonella infection in response to damage to the Salmonella-containing vacuole. *J Biol Chem* 2006; 281:11374-83; PMID:16495224; <http://dx.doi.org/10.1074/jbc.M509157200>
- [11] Meijer AJ, Codogno P. Signalling and autophagy regulation in health, aging and disease. *Mol Aspects Med* 2006; 27:411-25; PMID:16973212; <http://dx.doi.org/10.1016/j.mam.2006.08.002>
- [12] Thurston TL, Wandel MP, von Muhlinen N, Foeglein A, Randow F. Galectin 8 targets damaged vesicles for autophagy to defend cells against bacterial invasion. *Nature* 2012; 482:414-8; PMID:22246324; <http://dx.doi.org/10.1038/nature10744>
- [13] Delgado MA, Elmaoued RA, Davis AS, Kyei G, Deretic V. Toll-like receptors control autophagy. *EMBO J* 2008; 27:1110-21; PMID:18337753; <http://dx.doi.org/10.1038/emboj.2008.31>
- [14] Travassos LH, Carneiro LA, Ramjeet M, Hussey S, Kim YG, Magalhaes JG, Yuan L, Soares F, Chea E, Le Bourhis L, et al. Nod1 and Nod2 direct autophagy by recruiting ATG16L1 to the plasma membrane at the site of bacterial entry. *Nat Immunol* 2010; 11:55-62; PMID:19898471; <http://dx.doi.org/10.1038/ni.1823>
- [15] Tang D, Kang R, Coyne CB, Zeh HJ, Lotze MT. PAMPs and DAMPs: signal 0s that spur autophagy and immunity. *Immunol Rev* 2012; 249:158-75; PMID:22889221; <http://dx.doi.org/10.1111/j.1600-065X.2012.01146.x>
- [16] Levine B, Deretic V. Unveiling the roles of autophagy in innate and adaptive immunity. *Nat Rev Immunol* 2007; 7:767-77; PMID:17767194; <http://dx.doi.org/10.1038/nri2161>
- [17] Djavaheri-Mergny M, Amelotti M, Mathieu J, Besancon F, Bauvy C, Souquere S, Pierron G, Codogno P. NF-kappaB activation represses tumor necrosis factor-alpha-induced autophagy. *J Biol Chem* 2006; 281:30373-82; PMID:16857678; <http://dx.doi.org/10.1074/jbc.M602097200>
- [18] Helmy KY, Katschke KJ Jr, Gorgani NN, Kljavin NM, Elliott JM, Diehl L, Scales SJ, Ghilardi N, van Lookeren Campagne M. CRlg: a macrophage complement receptor required for phagocytosis of circulating pathogens. *Cell* 2006; 124:915-27; PMID:16530040; <http://dx.doi.org/10.1016/j.cell.2005.12.039>
- [19] Kim JK, Choi EM, Shin HI, Kim CH, Hwang SH, Kim SM, Kwon BS. Characterization of monoclonal antibody specific to the Z39Ig protein, a member of immunoglobulin superfamily. *Immunol Lett* 2005; 99:153-61; PMID:16009265; <http://dx.doi.org/10.1016/j.imlet.2005.02.012>
- [20] Kim KH, Choi BK, Song KM, Cha KW, Kim YH, Lee H, Han IS, Kwon BS. CRlg signals induce anti-intracellular bacterial phagosome activity in a chloride intracellular channel 3-dependent manner. *Eur J Immunol* 2013; 43:667-78; PMID:23280470; <http://dx.doi.org/10.1002/eji.201242997>
- [21] Vogt L, Schmitz N, Kurrer MO, Bauer M, Hinton HI, Behnke S, Gatto D, Sebbel P, Beerli RR, Sonderegger I, et al. VSIG4, a B7 family-related protein, is a negative regulator of T cell activation. *J Clin Invest* 2006; 116:2817-26; PMID:17016562; <http://dx.doi.org/10.1172/JCI25673>
- [22] Katschke KJ Jr, Helmy KY, Steffek M, Xi H, Yin J, Lee WP, Gribling P, Barck KH, Carano RA, Taylor RE, et al. A novel inhibitor of the alternative pathway of complement reverses inflammation and bone destruction in experimental arthritis. *J Exp Med* 2007; 204:1319-25; PMID:17548523; <http://dx.doi.org/10.1084/jem.20070432>
- [23] Tanida I, Minematsu-Ikeguchi N, Ueno T, Kominami E. Lysosomal turnover, but not a cellular level, of endogenous LC3 is a marker for autophagy. *Autophagy* 2005; 1:84-91; PMID:16874052; <http://dx.doi.org/10.4161/auto.1.2.1697>
- [24] Shang L, Chen S, Du F, Li S, Zhao L, Wang X. Nutrient starvation elicits an acute autophagic response mediated by Ulk1 dephosphorylation and its subsequent dissociation from AMPK. *Proc Natl Acad Sci U S A* 2006; 103:1107-12; PMID:16530040; <http://dx.doi.org/10.1073/pnas.0510110103>

- Sci U S A 2011; 108:4788-93; PMID:21383122; <http://dx.doi.org/10.1073/pnas.1100844108>
- [25] Yamamoto A, Tagawa Y, Yoshimori T, Moriyama Y, Masaki R, Tashiro Y. Bafilomycin A1 prevents maturation of autophagic vacuoles by inhibiting fusion between autophagosomes and lysosomes in rat hepatoma cell line, H-4-II-E cells. *Cell Struct Funct* 1998; 23:33-42; PMID:9639028; <http://dx.doi.org/10.1247/csf.23.33>
- [26] Mizushima N. Methods for monitoring autophagy. *Int J Biochem Cell Biol* 2004; 36:2491-2502; PMID:15325587; <http://dx.doi.org/10.1016/j.biocel.2004.02.005>
- [27] Kang R, Zeh HJ, Lotze MT, Tang D. The Beclin 1 network regulates autophagy and apoptosis. *Cell Death Differ* 2011; 18:571-80; PMID:21311563; <http://dx.doi.org/10.1038/cdd.2010.191>
- [28] Kim J, Kim YC, Fang C, Russell RC, Kim JH, Fan W, Liu R, Zhong Q, Guan KL. Differential regulation of distinct Vps34 complexes by AMPK in nutrient stress and autophagy. *Cell* 2013; 152:290-303; PMID:23332761; <http://dx.doi.org/10.1016/j.cell.2012.12.016>
- [29] Sanger JM, Chang R, Ashton F, Kaper JB, Sanger JW. Novel form of actin-based motility transports bacteria on the surfaces of infected cells. *Cell Motil Cytoskeleton* 1996; 34:279-87; PMID:8871815
- [30] Porte F, Naroeni A, Ouahrani-Bettache S, Liautard JP. Role of the *Brucella suis* lipopolysaccharide O antigen in phagosomal genesis and in inhibition of phagosome-lysosome fusion in murine macrophages. *Infect Immun* 2003; 71:1481-90; PMID:12595466; <http://dx.doi.org/10.1128/IAI.71.3.1481-1490.2003>
- [31] Bampton ET, Goemans CG, Niranjana D, Mizushima N, Tolkovsky AM. The dynamics of autophagy visualized in live cells: from autophagosome formation to fusion with endo/lysosomes. *Autophagy* 2005; 1:23-36; PMID:16874023; <http://dx.doi.org/10.4161/autol.1.1.1495>
- [32] Mizushima N, Noda T, Yoshimori T, Tanaka Y, Ishii T, George MD, Klionsky DJ, Ohsumi M, Ohsumi Y. A protein conjugation system essential for autophagy. *Nature* 1998; 395:395-8; PMID:9759731; <http://dx.doi.org/10.1038/26506>
- [33] Kraft C, Peter M, Hofmann K. Selective autophagy: ubiquitin-mediated recognition and beyond. *Nat Cell Biol* 2010; 12:836-41; PMID:20811356; <http://dx.doi.org/10.1038/ncb0910-836>
- [34] Dortet L, Mostowy S, Samba-Louaka A, Gouin E, Nahori MA, Wiemer EA, Dussurget O, Cossart P. Recruitment of the major vault protein by InlK: a *Listeria monocytogenes* strategy to avoid autophagy. *PLoS Pathog* 2011; 7:e1002168; PMID:21829365; <http://dx.doi.org/10.1371/journal.ppat.1002168>
- [35] Yoshikawa Y, Ogawa M, Hain T, Yoshida M, Fukumatsu M, Kim M, Mimuro H, Nakagawa I, Yanagawa T, Ishii T, Kakizuka A, Sztul E, Chakraborty T, Sasakawa C. *Listeria monocytogenes* ActA-mediated escape from autophagic recognition. *Nat Cell Biol*. 2009; 11:1233-40; PMID:19749745; <http://dx.doi.org/10.1038/ncb1967>
- [36] Tattoli I, Sorbara MT, Yang C, Tooze SA, Philpott DJ, Girardin SE. *Listeria* phospholipases subvert host autophagic defenses by stalling pre-autophagosomal structures. *EMBO J* 2013; 32:3066-78; PMID:24162724; <http://dx.doi.org/10.1038/emboj.2013.234>
- [37] Ogawa M, Yoshikawa Y, Mimuro H, Hain T, Chakraborty T, Sasakawa C. Autophagy targeting of *Listeria monocytogenes* and the bacterial countermeasure. *Autophagy* 2011; 7:310-4; PMID:21193840; <http://dx.doi.org/10.4161/autol.7.3.14581>
- [38] Gutierrez MG, Master SS, Singh SB, Taylor GA, Colombo MI, Deretic V. Autophagy is a defense mechanism inhibiting BCG and *Mycobacterium tuberculosis* survival in infected macrophages. *Cell* 2004; 119:753-66; PMID:15607973; <http://dx.doi.org/10.1016/j.cell.2004.11.038>
- [39] Delgado MA, Elmaoued RA, Davis AS, Kyei G, Deretic V. Toll-like receptors control autophagy. *EMBO J* 2008; 27:1110-21; PMID:18337753; <http://dx.doi.org/10.1038/emboj.2008.31>
- [40] Shi CS, Kehrl JH. MyD88 and Trif target Beclin 1 to trigger autophagy in macrophages. *J Biol Chem* 2008; 283:33175-82; PMID:18772134; <http://dx.doi.org/10.1074/jbc.M804478200>
- [41] Vural A, Kehrl JH. Autophagy in macrophages: impacting inflammation and bacterial infection. *Scientifica (Cairo)* 2014; 2014:825463; PMID:24818040; <http://dx.doi.org/10.1155/2014/825463>
- [42] Lee MY, Kim WJ, Kang YJ, Jung YM, Kang YM, Suk K, Park JE, Choi EM, Choi BK, Kwon BS, Lee WH. Z391g is expressed on macrophages and may mediate inflammatory reactions in arthritis and atherosclerosis. *J Leukoc Biol* 2006; 80:922-8; PMID:16882875; <http://dx.doi.org/10.1189/jlb.0306160>
- [43] Warner N, Nunez G. MyD88: a critical adaptor protein in innate immunity signal transduction. *J Immunol* 2013; 190(1):3-4; PMID:23264668; <http://dx.doi.org/10.4049/jimmunol.1203103>
- [44] Joubert PE, Meiffren G, Gregoire IP, Pontini G, Richetta C, Flacher M, Azocar O, Vidalain PO, Vidal M, Lotteau V, Codogno P, Rabourdin-Combe C, Faure M. Autophagy induction by the pathogen receptor CD46. *Cell Host Microbe* 2009; 6(4):354-66; PMID:19837375; <http://dx.doi.org/10.1016/j.chom.2009.09.006>
- [45] Liao Y, Guo S, Chen Y, Cao D, Xu H, Yang C, Fei L, Ni B, Ruan Z. VSIG4 expression on macrophages facilitates lung cancer development. *Lab Invest* 2014; 94:706-15; PMID:24862966; <http://dx.doi.org/10.1038/labinvest.2014.73>
- [46] MacGowan AP, Peterson PK, Keane W, Quie PG. Human peritoneal macrophage phagocytic, killing, and chemiluminescent responses to opsonized *Listeria monocytogenes*. *Infect Immun* 1983; 40:440-3; PMID:6403471; <http://iai.asm.org/content/40/1/440.long>
- [47] Cho SW, Kim S, Kim JM, Kim JS. Targeted genome engineering in human cells with the Cas9 RNA-guided endonuclease. *Nat Biotechnol* 2013; 31:230-2; PMID:23360966; <http://dx.doi.org/10.1038/nbt.2507>
- [48] Ramakrishna S, Kwaku Dad AB, Beloor J, Gopalappa R, Lee SK, Kim H. Gene disruption by cell-penetrating peptide-mediated delivery of Cas9 protein and guide RNA. *Genome Res* 2014; 24:1020-7; PMID:24696462; <http://dx.doi.org/10.1101/gr.171264.113>